INTERNATIONAL JOURNAL OF COMPUTERS COMMUNICATIONS & CONTROL
Online ISSN 1841-9844, ISSN-L 1841-9836, Volume: 18, Issue: 5, Month: October, Year: 2023
Article Number: 5630, https://doi.org/10.15837/ijccc.2023.5.5630

CCC Publications

RST Switching Bi-controller Based Flatness for an Electronic Throttle Valve

H. Gharsallaoui, W. Gritli, M. Benrejeb, P. Borne

Hajer Gharsallaoui, Wafa Gritli, Mohamed Benrejeb
Tunis El Manar University, National School of Engineers of Tunis, Tunisia.
hajer.gharsallaoui@eniso.u-sousse.tn, wafa.gritli@enit.rnu.tn, mohamed.benrejeb@enit.utm.tn

Pierre Borne
University of Lille, CNRS, Ecole Centrale Lille, UMR 9189, CRIStAL, Lille, France.
pierre.borne@univ-lille.fr

Abstract

In this paper, an RST switching bi-controller, based on flatness and on Luenberger observers, is designed to control the opening angle change of an Electronic Throttle Valve (ETV), to compensate unexpected external disturbances and to detect sensor faults. Two identified mathematical linear models are established to simulate the ETV for two different positions of the throttle plate. The use of robust RST switching bi-controller based-flatness approach by the development of closed-loop control is proposed, in order to obtain a stable system tracking a desired flat trajectory. The switching between the two models using stateflow tool is based on residual values generated by using the Luenberger observers in order to detect and to localize sensor faults occurrence. The observer's gains are determined using Linear Matrix Inequalities (LMIs) taking into account the stability of the system based on Lyapunov theory. The simulation results show the efficiency of the developed robust switching RST bi-controller based-flatness in terms of tracking the desired angle's reference trajectory, rejecting disturbances and detecting sensor faults.
Keywords: Electronic throttle valve, RST switching bi-controller, flatness, Luenberger observers, LMIs, sensor fault detection.

1 Introduction

It's worth mentioning that the majority of automotive engines are using the ETV in order to control the airflow rate of the internal combustion by regulating the throttle plate position, [1, 26, 30, 32, 35, 37, 38]. The throttle valve is composed by a throttle plate and a motor which forces the plate to rotate to a defined angle and then to return to its original position, due to the presence of a spring. The throttle plate is responsible for regulating the amount of air that flows into the engine. Its primary purpose is to modify the air-fuel mixture by altering the valve plate's opening angle, which controls the airflow into the engine during combustion. The control of the throttle plate, specifically its angular position, has a direct impact on the efficiency and on emissions of the engine. The throttle plate's angular position has to follow a desired trajectory, as determined by an accelerator pedal, to correspond to the current engine load. It results in enhancements in vehicle drivability, fuel efficiency and safety [1, 26, 32, 35, 37, 38]. Several control strategies have been proposed in the literature for complex dynamic systems [8] and especially to control the electronic throttle, including the Proportional-Integral-Derivative (PID) controller and a feedback compensator for friction and limp-home effects as discussed in [12]. A similar study, presented in [14], tackled an experimental benchmark of robust control of throttle valve positions. Moreover, a sliding mode controller, based on observer in discrete-time framework, were designed in order to obtain a robust tracking control of the valve system in [4, 13]. Furthermore, in [41] is introduced an Adaptive Inverse Model Control System (AIMCS) for the ETV, which employs two radial basis function neural networks. Differential flatness [16, 18, 19, 20] was previously used for trajectory planning and tracking control [2, 17], with controller-based flatness designed specifically for the ETV. In [42], an adaptive backstepping sliding mode control based on the Radial Basis Function Neural Network (RBFNN) was proposed for vehicle's wheel slip tracking. Referring to [24, 35], the diagnosis of gasoline injection engines and fault tolerant control based on fuzzy logic control were studied. In reference [5], an engine's ETV position estimation was achieved through the use of a neural network-based virtual sensor. Meanwhile, [38] aimed to enhance the performance of the electronic throttle control through hybrid theory-based time-optimal control. For more details about ETVs, a comprehensive description of later trends in the design and verification/validation of ETV-based modern systems can be found in [1]. Otherwise, a great part of the research community was tackled the control issues linked to ETVs. In [7, 11, 15, 22, 27, 28, 29, 31, 34], multi-model approaches for complex systems modeling based on unconventional strategies such as genetic algorithms and fuzzy control are proposed. In this context and in order to present advanced ETV control approaches, the work depicted in [25] studied the impact of nonlinearities in the ETV system and its parameters through the heuristic genetic algorithm based on flatness control. A Takagi-Sugeno fuzzy control strategy for automotive ETVs under the presence of unknown inputs was elaborated in [24]. Barrier Lyapunov function-based adaptive backstepping control for Electronic Throttle Control Systems (ETCS) is designed to track the desired throttle angle [39]. A similar work, presented in [33], proposed an asymmetric modeling and control for ETVs. Chaos control and stability analysis of an ETV dynamical system were introduced in [10]. More interest should be dedicated to propose suitable control methods for such widespread systems in terms of tracking desired trajectory in presence of faults. Certainly, tackling only the design/implementation, verification/validation, controllability or the energy efficiency issues is not sufficient for ETVs. Even within an optimal control scheme [38], an appropriate operation of ETVs is not possible under fault occurrences. Such an issue has not been sufficiently studied in the literature [35, 36]. More interest should be dedicated to suggest specific diagnosis methods for such systems.

In this paper, a robust RST switching bi-controller, based on flatness and on Luenberger observers, of the ETV is put forward. The flatness property is proposed to define a desired output reference trajectory starting from a flat output system. The use of this property concerns the elaboration of the control in a closed loop, in order to obtain a stable system tracking a desired trajectory in a discrete-time formalism. A set of Luenberger observers is designed to estimate the system states in order to generate residual values. A switching strategy using stateflow based on residual values evaluation, that allows the selection of the appropriate RST based flatness controller in presence of sensor fault, is proposed. LMIs approaches are employed in order to ensure ETV system stability.

This paper is organized as follows. In section II, the design of the proposed RST bi-controller and the switching approach between the two ETV models, based on residual value, are provided. In section III, a robust RST bi-controller based on flatness and on Luenberger observers considering the sensor fault detection occurrence is put forward. The application of the RST switching bi-controller based flatness to the ETV and corresponding simulation results, emphasizing the efficiency of the proposed approach are presented in Section VI.

2 Proposed ETV RST bi-controller

2.1 Basic idea

In previous works [16, 17, 18, 19, 20, 21], it has been shown that flatness control provides higher performance than conventional control systems in term of tracking of the desired reference trajectory starting from a flat output system.

Furthermore, as advantage of the proposed approach of control, the addition of Luenberger observers, for ETV's parameters estimation, makes the control system more robust. Also, Luenberger observers are designed to detect and to localize sensor fault based on residual values comparison.

The performances obtained by switching, in terms of tracking of the desired angle's trajectory and sensor faults rejection, are proposed in this paper. Besides, this novel control approach applied for ETV system takes into account the stability analysis of a switching control strategy based on Lyapunov function.

Moreover, as another significant advantage, the proposed RST based-flatness bi-controller ensures the maintain of nominal performances as well as the noise suppression and the attenuation of the input/output disturbances in high frequencies.

However, the objective of the present work is to design a robust RST bi-controller structure for an ETV, described by two operating models. The switching between the two models is based actually on comparing the residues between the model estimated output calculated using a Luenberger observer and the real one of the system.

Two RST flatness-based controllers C_1 and C_2 are designed specifically for two given models H_1 and H_2 of the ETV process as mentioned in reference [17, 40]. The stateflow tool in MATLAB/Simulink is proposed to select between the control signal $u_1(k)$ or $u_2(k)$, which corresponds to the smallest residue. Referring to [7, 11, 28, 29, 34], switching control approaches are suggested for complex systems based on multi-model formalism. To determine the appropriate controller and timing for switching between controllers, a switching approach control is presented below.

1) Flatness-based RST bi-controllers C_1 and C_2 are designed, respectively, for operating models H_1 and H_2, for $j \in \{1, 2\}$, for which the transfer functions of the open-loop discrete-time process are in the form

$$H_j(q^{-1}) = \frac{B_j(q^{-1})}{A_j(q^{-1})} \tag{1}$$

with

$$A_j(q^{-1}) = 1 + a_{j,n-1}q^{-1} + \ldots + a_{j,1}q^{-n+1} + a_{j,0}q^{-n} \tag{2}$$

$$B_j(q^{-1}) = b_{j,n-1}q^{-1} + \ldots + b_{j,1}q^{-n+1} + b_{j,0}q^{-n} \tag{3}$$

$a_{j,i}$ and $b_{j,i}$ constant parameters, $i = 0, 1, ..., n-1$ and q^{-1} the causal operator.

The proposed RST flatness-based control approach is firstly developed in a discrete-time framework in order to track a reference trajectory starting from flat outputs system $z_j(k)$. Then, the planning of the desired flat trajectories $z_j^d(k)$ for flat output system variables $z_j(k)$ is established.

2) The choice of the polynomial $K(q)$, the denominator of the tracking dynamic, is performed such that closed-loop poles should be well optimized in order to satisfy the desired performances of the proposed ETV RST based-flatness bi-controller. Indeed, the design of the proposed controller is guided by the choice of the tracking polynomial $K(q)$.

Let's consider $d(t)$ and $f(t)$, respectively, the unexpected disturbance and the sensor fault.

3) For the models H_1 and H_2, corresponding Luenberger observers L_1 and L_2 are introduced, as shown in Figure 1.

4) Residual value $r_1(k)$ (respectively $r_2(k)$) is generated for the operating models H_1 (respectively H_2). They will be used to detect the sensor fault.

$$r_1(k) = y(k) - \hat{y}_1(k) \tag{4}$$

$$r_2(k) = y(k) - \hat{y}_2(k) \tag{5}$$

$\hat{y}_1(k)$ and $\hat{y}_2(k)$ are the estimated outputs, respectively, of operating models H_1 and H_2. While, the residual values $r_j(k)$ represent the difference between the real system output $y(k)$ and the estimated

outputs $\hat{y}_j(k)$ for each model.
5) The controller selection is based on residues using a stateflow modelling tool described in paragraph (2.2), where the selected RST based-flatness controller C_1 or C_2 corresponds to the argument with the smallest residual value using a transition method, [18, 19, 20, 21].
6) The residue value index determines the appropriate desired flat trajectory $z_1^d(k)$ or $z_2^d(k)$, corresponding to the active operator mode H_1 or H_2.
7) The control signal $u_j(k)$, generated by the selected active controller C_1 or C_2, is used to control model H_1 or H_2.
8) The tracking errors $e_j(k)$, $j = 1, 2$, are the difference between the real system output $y(k)$ and the desired outputs $y_j^d(k)$ for each operating model.

$$e_j(k) = y(k) - y_j^d(k) \tag{6}$$

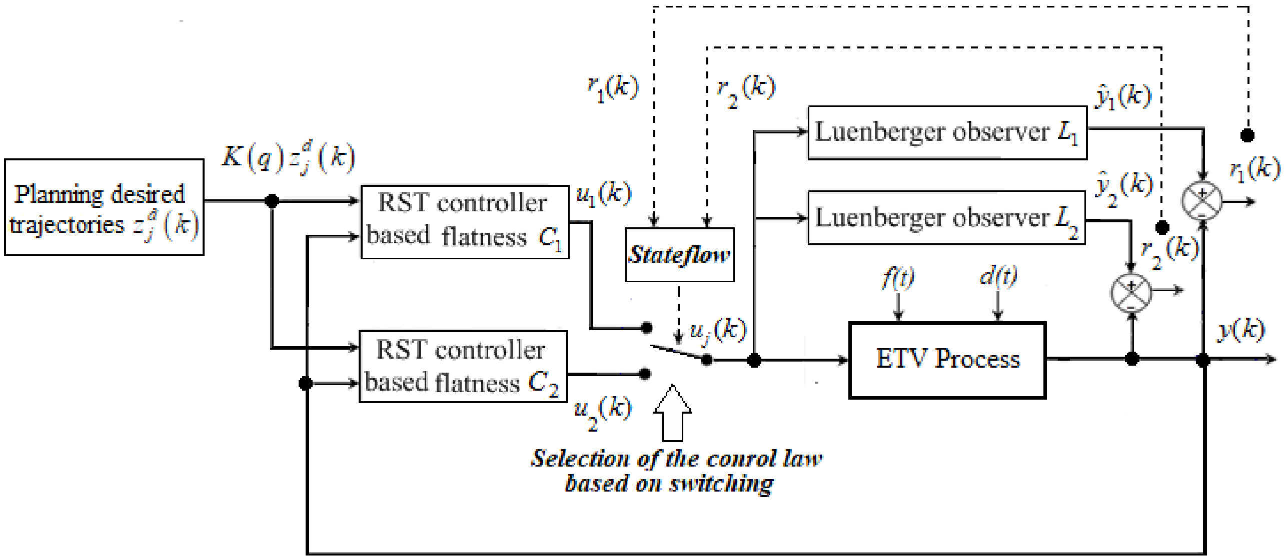

Figure 1: Proposed RST flatness-based bi-controller structure using Luenberger observers based on residual values

Among the existing linear model-based fault-tolerant control schemes, we find the so-called observer-based technique. This technique has been developed for advanced control theory, where observers are considered as powerful tools for variables efficient estimation and for faults detection. In our case of study, Luenberger observers are used for linear models in order to estimate system parameters as well as to detect sensor fault by analysing the residues which are the difference between the measured process variables and their estimates. Indeed, a residual signal presents the most important criterion for an efficient fault detection method.
The proposed ETV switching RST bi-controller based on flatness and on Luenberger observers, in order to adjust the throttle angular position, is based on a simple reconfiguration structure control consisting of two combined parts. The first is dedicated to the detection of the operating mode process, while the second is for the decision to select the right controller. The ETV process is therefore controlled by the signal issued by the active controller. This switching strategy is described in the next subsection.

2.2 Switching strategy

In the context of multi-model formalism, the purpose is to pinpoint the faulty operating model. In fact, multiple model-based diagnosis approaches are used frequently. Nowadays, various model-based diagnosis techniques are commonly employed, whereby an operating model of the system under control is used to compute residuals [19, 20, 21]. The residue is the difference between the measured process variables and their estimates. Indeed, a residual signal presents the most important criterion for an

efficient fault reconfiguration control. If the residual exceeds a predefined threshold, then there is a fault occurrence. Else, it is fault free. A stateflow diagram consists of states, transitions and events which are used to model the behavior of the studied ETV system. States present the evolution of the two operating models H_1 and H_2 of ETV system, transitions represent the conditions of switching between states obtained by the comparison between the residues of operating models and events represent the selection of the argument of the smallest residue that causes the transition between states. The following four steps outline a detection method used to decide when and to which controller one should switch for the case of RST bi-controller based on Luenberger observers:
1) Simulate the two models H_1 and H_2.
2) Evaluate the residues $r_1(k)$ and $r_2(k)$ issued from the corresponding Luenberger observers, characterized, respectively, by L_1 and L_2 for each operating model output.
3) Represent and simulate the stateflow with the two models H_1 and H_2 and the transitions by establishing the logic decision using state machines and flow charts, as illustrated in Figure 2.
4) Select and transfer the smallest residual value index to the state flow chart tool that enables the control decision. The following detection rule $det(k)$, computed on-line, decides that the process D is operating in the m^{th} mode H_m at each sampling period T_e

$$det(k) = \{D = H_m,\ m = arg\ min\ r_j(k),\ j = 1, 2\} \tag{7}$$

Thus, the j^{th} selected controller and the j^{th} appropriate flat desired trajectory correspond to the j^{th} argument of the smallest residue.

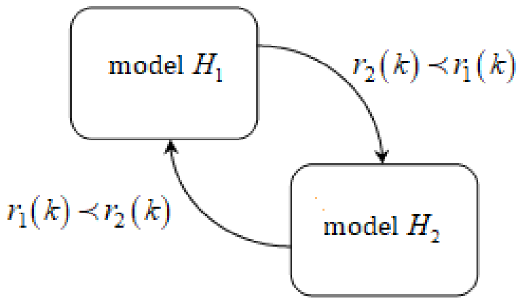

Figure 2: Stateflow modelling for two models

3 Proposed robust RST bi-controller based-flatness design

The concept of flatness, initially introduced in [16] for nonlinear continuous-time systems, was extended to discrete-time systems [18, 19, 20, 21] to design control approaches that ensure the tracking of a desired reference trajectory. The most important significant advantage of differential flatness is that it enables the direct representation of state and input variables in terms of a flat output and a finite number of its derivatives, without requiring the integration of any differential equation [16]. As investigated in this paper, the important benefit of using flatness is its efficiency in trajectory planning with accuracy.

3.1 Flatness and trajectory planning preliminaries

(a) Flatness

To implement a robust bi-controller, the flatness approach is used in a discrete-time formalism. For $j \in \{1, 2\}$, let's consider the studied dynamic linear discrete-time system described by

$$A_j(q^{-1})y_j(k) = B_j(q^{-1})u_j(k) \tag{8}$$

$u_j(k)$ and $y_j(k)$ are the input and the output, respectively, $A_j(q^{-1})$ and $B_j(q^{-1})$, the polynomials already defined in (2) and (3).

The parameters $a_{j,i}$ and $b_{j,i}$ are constants, $i = 0, 1, ..., n-1$ and q^{-1} is the causal operator. According to [16, 18, 19, 20, 21], the discrete flat output $z_j(k)$ of a dynamic system can be considered as the partial state and expressed as a function of the input $u_j(k)$ and the output signals $y_j(k)$ as follows

$$u_j(k) = A_j(q^{-1})z_j(k) \tag{9}$$

$$y_j(k) = B_j(q^{-1})z_j(k) \tag{10}$$

Referring to [18, 19, 20, 21], if the actual output signal $y_j(k)$, to be controlled, is not a flat output, it becomes necessary to determine a desired trajectory planning for the flat output and subsequently to consider relation (10).

(b) Trajectory planning

The control output variable $u_j^d(t)$ must be written as the function of the flat output $y_j^d(t)$ and their derivatives. The relations below can be used to determine the control law [18, 19, 20, 21] for $j \in \{1, 2\}$.

$$u_j^d(t) = h(z_j^d(t), ..., z_j^{d(\alpha+1)}(t)) \tag{11}$$

$$y_j^d(t) = g(z_j^d(t), ..., z_j^{d(\sigma)}(t)) \tag{12}$$

with h and g vectorial functions and z_j^d the desired trajectory for the continuous-time flat output that must be $sup(\alpha + 1, \sigma)$ time continuously derivable.

To plan the desired flat trajectory $z_j^d(t)$, the polynomial interpolation technique is employed. The state vector $Z_j^d(t)$ represents the desired continuous flat output and its successive derivatives.

The two times t_0 and t_f are pre-determined and the expression of $Z_j^d(t)$, for $j \in \{1, 2\}$, can be obtained using the method presented in [18, 19, 20, 21]; it comes

$$Z_1^d(t) = M_{1,1}(t - t_0)c_{1,1}(t_0) + M_{1,2}(t - t_0)c_{1,2}(t_0, t_f) \tag{13}$$

$$Z_2^d(t) = M_{2,1}(t - t_0)c_{2,1}(t_0) + M_{2,2}(t - t_0)c_{2,2}(t_0, t_f) \tag{14}$$

with matrices $M_{1,1}$, $M_{2,1}$, $M_{1,2}$ and $M_{2,2}$ defined by

$$M_{1,1} = \begin{pmatrix} 1 & t \\ 0 & 1 \end{pmatrix} \tag{15}$$

$$M_{2,1} = \begin{pmatrix} 1 & t \\ 0 & 1 \end{pmatrix} \tag{16}$$

$$M_{1,2} = \begin{pmatrix} \frac{t^2}{(2)!} & \frac{t^3}{(3)!} \\ t & \frac{t^2}{(2)!} \end{pmatrix} \tag{17}$$

$$M_{2,2} = \begin{pmatrix} \frac{t^2}{(2)!} & \frac{t^3}{(3)!} \\ t & \frac{t^2}{(2)!} \end{pmatrix} \tag{18}$$

and vectors $c_{1,1}$, $c_{2,1}$, $c_{1,2}$ and $c_{2,2}$ by

$$c_{1,1} = Z_1^d(t_0) \tag{19}$$

$$c_{2,1} = Z_2^d(t_0) \tag{20}$$

$$c_{1,2} = M_{1,2}^{-1}(t_f - t_0)(Z_1^d(t_f) - M_{1,1}(t_f - t_0)Z_1^d(t_0)) \tag{21}$$

$$c_{2,2} = M_{2,2}^{-1}(t_f - t_0)(Z_2^d(t_f) - M_{2,1}(t_f - t_0)Z_2^d(t_0)) \tag{22}$$

Once the flat trajectory $z_j^d(k)$ is planned, the corresponding desired output trajectory $y_j^d(k)$ is established. In the discrete-time context, the actual output of system $y_j(k)$ to be controlled, tracks asymptotically the desired trajectory $y_j^d(k)$ expressed by

$$y_j^d(k) = B_j(q^{-1})z_j^d(k) \tag{23}$$

$z_j^d(k)$ are the values of the continuous-time trajectory $z_j^d(t)$ at k sampling instant.

3.2 RST bi-controller structure

Flatness, developed initially for nonlinear systems, has been adapted for both finite dimensional linear systems in both continuous-time and discrete-time cases then extended to infinite-dimensional systems. This section outlines the application of RST bi-controller based-flatness to linear systems. In order to implement an RST bi-controller based-flatness for the open-loop discrete-time process described by the transfer function (1), a direct computing approach is used for the state vector as below [18]

$$Z_j(k) = \begin{pmatrix} z_j(k) & z_j(k+1) & \cdots & z_j(k+n-1) \end{pmatrix}^T \tag{24}$$

It comes the controllable form of the system's state space description

$$\begin{cases} Z_j(k+1) = \mathbf{A}_j Z_j(k) + \mathbf{B}_j u_j(k) \\ y_j(k) = \mathbf{C}_j Z_j(k) \end{cases} \tag{25}$$

with $Z_j(k) \in \mathbb{R}^n$ the state vector, $u_j(k) \in \mathbb{R}^p$ the input vector, $y_j(k) \in \mathbb{R}^m$ the measure vector, and $\mathbf{A}_j \in \mathbb{R}^{n\times n}$, $\mathbf{B}_j \in \mathbb{R}^{n\times p}$ and $\mathbf{C}_j \in \mathbb{R}^{m\times n}$ the known constant matrices, for $j \in \{1, 2\}$, given by

$$\mathbf{A}_j = \begin{pmatrix} 0 & 1 & 0 & \cdots & 0 \\ 0 & 0 & 1 & \ddots & \vdots \\ \vdots & \ddots & \ddots & \ddots & 0 \\ 0 & \cdots & 0 & 0 & 1 \\ -a_{j,0} & -a_{j,1} & \ldots & -a_{j,n-2} & -a_{j,n-1} \end{pmatrix} \tag{26}$$

$$\mathbf{C}_j = \begin{pmatrix} b_{j,0} & b_{j,1} & \cdots & b_{j,n-1} \end{pmatrix} \tag{27}$$

$$\mathbf{B}_j = \begin{pmatrix} 0 & 0 & \cdots & 0 & 1 \end{pmatrix}^T \tag{28}$$

Then, the control law, based flatness, can be expressed as, [18, 19, 20, 21]

$$u_j(k) = K(q) z_j^d(k) + (a - k) Z_j(k) \tag{29}$$

The constant components of the vectors a and k are the coefficients $a_{j,i}$ and k_i of the polynomials, respectively, $A_j(q^{-1})$ and $K(q)$

$$a = (a_{j,0} \quad a_{j,1} \quad \cdots \quad a_{j,n-1}) \tag{30}$$

$$k = (k_0 \quad k_1 \quad \cdots \quad k_{n-1}) \tag{31}$$

The polynomial $K(q)$ is the denominator of the tracking dynamic which is a discrete-time 4^{th} order model equivalent to a continuous-time one $G_d(s)$ composed by the cascading of two continuous-time systems. The first system $G_{d_1}(s)$ is a second order with fixed damping factor ξ and fixed frequency ω_0 given by (32). Whereas, the second system $G_{d_2}(s)$ is a second order model with a fixed time constant τ, given by (33), where s is the Laplace operator.

$$G_{d_1}(s) = \frac{\omega_0^2}{(s^2 + 2\omega_0 \xi s + \omega_0^2)} \tag{32}$$

$$G_{d_2}(s) = \frac{1}{(1 + \tau s)^2} \tag{33}$$

$$G_d(s) = \frac{\omega_0^2}{K(s)} \tag{34}$$

with

$$K(s) = (s^2 + 2\omega_0 \xi s + \omega_0^2)(1 + \tau s)^2 \tag{35}$$

$K(q)$ is a polynomial containing the closed loop poles. The dynamics of the closed-loop are defined by the tracking polynomial $K(q^{-1})$ such as [18, 19, 20, 21]

$$A_j(q^{-1})S_j(q^{-1}) + B_j(q^{-1})R_j(q^{-1}) = K(q^{-1}) \tag{36}$$

The choice of closed-loop poles of the polynomial $K(q)$ must be well optimized in order to satisfy the desired performances. This step is the main contribution of the exploitation of the flatness property in the design of such robust RST based-flatness bi-controller. Indeed, the choice of the closed-loop poles corresponds to that of the tracking model of a desired trajectory and, more precisely, to the poles of the $K(q)$ polynomial.

The RST based-flatness bi-controller's structure can be, then, obtained by the following equation

$$S_j(q^{-1})u_j(k) = K(q)z_j^d(k) - R_j(q^{-1})y_j(k) \tag{37}$$

with

$$R_j\left(q^{-1}\right) = -\left(a-k\right)\mathbf{A}_j^{n-1}O^{-1}{}_{(\mathbf{A}_j,\mathbf{C}_j)}Q_q \tag{38}$$

$$S_j\left(q^{-1}\right) = 1 + \left(a-k\right)\left(\mathbf{A}_j^{n-1}O^{-1}{}_{(\mathbf{A}_j,\mathbf{C}_j)}M_{(\mathbf{A}_j,\mathbf{B}_j,\mathbf{C}_j)} - \begin{pmatrix}\mathbf{A}_j^{n-2}\mathbf{B}_j & \ldots & \mathbf{B}_j\end{pmatrix}\right)Q_q^* \tag{39}$$

and

$$Q_q = \begin{pmatrix} q^{-(n-1)} & q^{-(n-2)} & \cdots & q^{-1} & 1\end{pmatrix}^T, \quad Q_q^* = \begin{pmatrix} q^{-(n-1)} & q^{-(n-2)} & \cdots & q^{-1}\end{pmatrix}^T \tag{40}$$

From this representation, the state space vector becomes

$$Z_j(k) = O^{-1}{}_{(\mathbf{A}_j,\mathbf{C}_j)}\left(Y_j(k) - M_{(\mathbf{A}_j,\mathbf{B}_j,\mathbf{C}_j)}U_j(k)\right) \tag{41}$$

with

$$Y_j(k) = \begin{pmatrix} y_j(k) & y_j(k+1) & \cdots & y_j(k+n-1)\end{pmatrix}^T \tag{42}$$

and

$$U_j(k) = \begin{pmatrix} u_j(k) & u_j(k+1) & \cdots & u_j(k+n-2)\end{pmatrix}^T \tag{43}$$

$M_{(\mathbf{A}_j,\mathbf{B}_j,\mathbf{C}_j)}$ and $O_{(\mathbf{A}_j,\mathbf{C}_j)}$ are the controllability and observability matrices respectively, given by

$$M_{(\mathbf{A}_j,\mathbf{B}_j,\mathbf{C}_j)} = \begin{pmatrix} 0 & \cdots & \cdots & 0 \\ \mathbf{C}_j\mathbf{B}_j & \ddots & \ddots & \vdots \\ \mathbf{C}_j\mathbf{A}_j\mathbf{B}_j & \mathbf{C}_j\mathbf{B}_j & \ddots & \vdots \\ \vdots & \ddots & \ddots & 0 \\ \mathbf{C}_j\mathbf{A}_j^{n-2}\mathbf{B}_j & \cdots & \mathbf{C}_j\mathbf{A}_j\mathbf{B}_j & \mathbf{C}_j\mathbf{B}_j \end{pmatrix} \tag{44}$$

$$O_{(\mathbf{A}_j,\mathbf{C}_j)} = \begin{pmatrix} \mathbf{C}_j \\ \mathbf{C}_j\mathbf{A}_j \\ \vdots \\ \mathbf{C}_j\mathbf{A}_j^{n-1} \end{pmatrix} \tag{45}$$

The next subsection is dedicated to introduce the conventional Luenberger observers for the two considered linear models and to study the stability of the ETV system. In addition, LMIs based on candidate Lyapunov functions are also provided in order to guarantee the stability of the ETV system.

3.3 Luenberger observers design and stability analysis of ETV system

In this paper, for the proposed switching RST bi-controller based-flatness, the fault detection is based on Luenberger observers used to generate the residual values. The observer's gains are calculated using LMIs and consequently the stabiliy of the system is verified by determining a common Lyapunov function, [6]. Let the associated j^{th} Luenberger observer of the discrete-time linear system (25) given by

$$\begin{cases} \hat{Z}_j(k+1) = \mathbf{A}_j\hat{Z}_j(k) + \mathbf{B}_j u_j(k) + \mathbf{L}_j(y_j(k) - \hat{y}_j(k)) \\ \hat{y}_j(k) = \mathbf{C}_j\hat{x}_j(k) \end{cases} \tag{46}$$

The matrix $\mathbf{L}_j \in \mathbb{R}^{n\times m}$ is the observer gain for the j^{th} model.

Problem. The stability analysis of the overall system for arbitrary switching signals have to be checked by the choice of a common Lyapunov function [7].

Theorem[3]. Consider the system (25) and assume that the pairs $(\mathbf{A}_j, \mathbf{C}_j)$ are observable for $j \in \{1, 2\}$. If there exists a symmetrical positive definite matrix P as the solution of the algebraic Lyapunov inequalities

$$(\mathbf{A}_j - \mathbf{L}_j\mathbf{C}_j)^T P(\mathbf{A}_j - \mathbf{L}_j\mathbf{C}_j) - P < 0, , \; j = 1, 2 \tag{47}$$

then, observer (46) involves an estimation error asymptotically convergent to zero.

Problem. Find $\mathbf{L}_j$ such that there exists a symmetric positive definite matrix P solving the Lyapunov inequalities (47). The above problem can be reduced to a simpler form that is well-suited to be solved by LMIs method [3] and [7]. To this end, let us consider the following lemma.

Lemma[2]. Given a symmetric positive definite matrix P, the inequality (47) is equivalent to (48) one,

$$\begin{pmatrix} P & P\mathbf{A}_j - Y_j\mathbf{C}_j \\ (P\mathbf{A}_j - Y_j\mathbf{C}_j)^T & P \end{pmatrix} > 0, \; j = 1, 2 \tag{48}$$

with

$$\mathbf{L}_j = P^{-1}Y_j \tag{49}$$

3.4 Sensor fault description

In general, the majority of dynamic systems are susceptible to fail and unforeseen behaviors. Thus, for security problem, many studies are proposed for detection and localization of the ETV faults. Consequently, it is crucial to promptly detect and pinpoint any disturbances or fault occurrence, allowing the necessity of diagnostic techniques.

In this context, we suggest an observer-based fault detection method for the ETV. The considered fault is sensor fault which is modeled by signals that are additive to the output signal. In the state space description (50)

$$\begin{cases} Z_j(k+1) = \mathbf{A}_j Z_j(k) + \mathbf{B}_j u_j(k) \\ y_j(k) = \mathbf{C}_j Z_j(k) + F_c f_c(t) \end{cases} \tag{50}$$

$f_c(t)$ represents the sensor faults and F_c the distribution matrix of sensor faults. Thus, the evaluation of residual values of the faulty system can indicate the occurrence of exogenous sensor faults.

4 Application to ETV

4.1 Studied ETV Modelling

In order to illustrate the effectiveness of the proposed RST bi-controller based-flatness, two linear models of the ETV of Figure 3, [40],[2] characterized by the parameters of Table 1, are considered.

The electrical part of the studied system is modeled by [40]

$$u(t) = Ri(t) + L\frac{d}{dt}i(t) + k_v\omega_m(t) \tag{51}$$

L is the inductance, R the resistance, $u(t)$ and $i(t)$ respectively, the control input voltage and the armature current, k_v the electromotive force constant and $\omega_m(t)$ the motor rotational speed.
The mechanical part of the throttle is modeled by

$$J\frac{d}{dt}\omega_m(t) = C_e - C_f - C_r - C_a \tag{52}$$

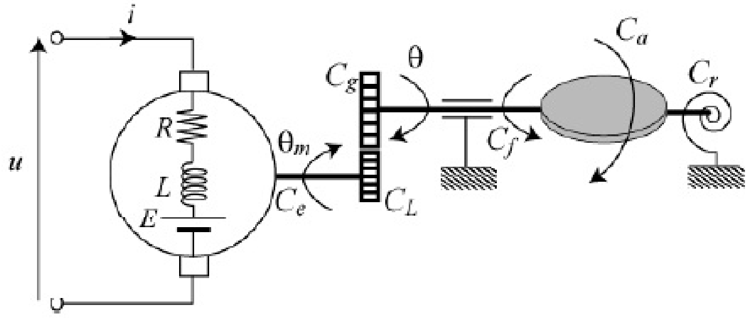

Figure 3: Studied ETV system [2]

and by

$$\frac{d}{dt}\theta(t) = (180/\pi/\gamma^*)\omega_m(t) \tag{53}$$

Its gear reducer is characterized by its reduction ratio γ^* such that

$$\gamma^* = C_g C_L^{-1} \tag{54}$$

with C_L the load torque, C_g the gear torque, $\theta(t)$ the throttle plate angle, J the overall moment of inertia, $C_e = k_e i(t)$ the electrical torque with constant k_e, C_f the torque caused by mechanical friction, C_r the spring resistive torque and C_a the torque generated by the airflow, [40] and [23].

The ETV involves two complex nonlinearities due to the nonlinear spring torque C_r and to the friction torque C_f. They are given by their following static characteristics [40]:

- the dead zone refers to a range where the nominal position of the valve plate remains unaffected by the control voltage signal,
- the valve plate's movement is restricted by a maximum and a minimum angles of θ, θ_{max} and θ_{min} respectively, resulting in the combination of two hysteresis effects and saturation.

The static characteristic of the nonlinear spring torque C_r is such that

$$C_r = \frac{k_r}{\gamma^*}(\theta - \theta_0) + D_s sgn(\theta - \theta_0) \tag{55}$$

with: $\theta_{\min} \leq \theta \leq \theta_{\max}$, k_r the spring constant, D_s a constant, θ_0 the default position and $sgn(,)$ the following signum function

$$sgn\,(\theta - \theta_0) = \begin{cases} 1, \text{if } \theta \geq \theta_0 \\ -1, \text{ else} \end{cases} \tag{56}$$

Then, the friction torque function C_f of the angular velocity of the throttle plate can be expressed as

$$C_f = f_v\omega + f_c sgn(\omega) \tag{57}$$

f_v and f_c are constant parameters.

By substituting in (52), the expressions of C_e, C_f and C_r and by neglecting the torque generated by airflow C_a, the two nonlinearities $sgn(\theta - \theta_0)$ and $sgn(\omega)$ and the two constants $k_r {\gamma^*}^{-1}\theta_0$ and $f_v\omega$, the transfer function of the linear model of the studied ETV becomes [40]

$$H(s) = \frac{(180/\pi/\gamma^*)k_e}{JLs^3 + JRs^2 + (k_e k_v + Lk_s)s + Rk_s} \tag{58}$$

with

$$k_s = (180/\pi/\gamma^{*2})k_r \tag{59}$$

Table 1: Model parameters given in ambient temperature of $25^{\circ}C$

Parameters	Values
R	2.8 (Ω)
L	0.0011 (H)
k_e	0.0183 (Nm/A)
k_v	0.0183 $(v/rad/s)$
J	4×10^{-6} $(kg.m^2)$
γ^*	16.95

The ETV is modeled by two linear models identified from the default position of the throttle plate where only the value of k_s varies, [40]. The system responses are obtained by the proposed RST bi-controller based-flatness approach from default position of the throttle angle $\theta_0 \simeq 0.22$ rad.

Depending on whether, the throttle plate is above or below the default position, then two transfer functions are obtained, [40].
Indeed, $H_1(s)$ represents the first continuous model that depicts the plate's position above default position, with a spring constant of k_s equal to $1.877 \times 10^{-4} kg.m^2$, [40].

$$H_1(s) = \frac{0.6186}{4.4.10^{-9}s^3 + 1.12.10^{-5}s^2 + 3.351.10^{-4}s + 5.256.10^{-4}} \tag{60}$$

Whereas, $H_2(s)$ represents the second continuous model that illustrates the throttle's position below default position, with a spring constant of k_s equal to $1.384 \times 10^{-3} kg.m^2$, [40].

$$H_2(s) = \frac{0.6186}{4.4.10^{-9}s^3 + 1.12.10^{-5}s^2 + 3.364.10^{-4}s + 3.875.10^{-4}} \tag{61}$$

The study was conducted with a sampling period $T_e = 0.002s$ [2], consequently, two mathematical linear models $H_1(q^{-1})$ and $H_2(q^{-1})$ are considered in discrete formalism, respectively, for the two models $H_1(s)$ and $H_2(s)$. Hence, the discrete-time transfer functions $H_1(q^{-1})$ and $H_2(q^{-1})$ are defined by their following expressions (62) and (63)

$$H_1(q^{-1}) = \frac{0.007480q^{-1} + 0.01334q^{-2} + 0.0007376q^{-3}}{1 - 1.948q^{-1} + 0.954q^{-2} - 0.006152q^{-3}} \tag{62}$$

$$H_2(q^{-1}) = \frac{0.007479q^{-1} + 0.01333q^{-2} + 0.0007376q^{-3}}{1 - 1.946q^{-1} + 0.954q^{-2} - 0.006152q^{-3}} \tag{63}$$

In the next paragraph, ETV RST bi-controllers based-flatness design is proposed for the predefined linear models $H_1(q^{-1})$ and $H_2(q^{-1})$ in the discrete-time framework.

4.2 ETV RST bi-controller based-flatness

The reference tracking model $G_d(s)$ corresponds to a fourth-order continuous-time system with a damping factor of $\xi = 0.8$, a natural frequency of $\omega_0 = 20\ rad/s$ and a time constant of τ =0.1 s.

The tracking polynomial $K(q)$ is defined by (64).

$$K(q) = q^4 - 3.897q^3 + 5.695q^2 - 3.699q + 0.9012 \tag{64}$$

The closed-loop poles of the tracking polynomial are well designed in order to satisfy performances of the proposed RST bi-controller based-flatness in terms of tracking of desired flat trajectory, disturbances rejection and noise attenuation.
Indeed, the poles of the desired polynomial $K(q)$ are: $p_{1,2} = 0.9682 \pm 0.0232i$ and $p_3 = p_4 = 0.9802$. The choice of these poles represents a compromise between the desired fast closed-loop response time and the robustness of the controllers to be calculated, which allows the sensitivity functions to be within the template. These poles are also used to define the disturbance rejection dynamics.

According to the equations (37) and (38), the RST bi-controller based-flatness yields the following polynomials

$$R_1(q^{-1}) = -0.5484 + 3.825q^{-1} - 5.899q^{-2} + 2.625q^{-3} \tag{65}$$

$$R_2(q^{-1}) = -2.115 + 6.897q^{-1} - 7.415q^{-2} + 2.634q^{-3} \tag{66}$$

$$S_1(q^{-1}) = 1 - 0.9496q^{-1} - 0.005625q^{-2} - 7.059 \times 10^{-6}q^{-3} \tag{67}$$

$$S_2(q^{-1}) = 1 - 0.9506q^{-1} - 0.006032q^{-2} - 2.723 \times 10^{-5}q^{-3} \tag{68}$$

After establishing of the RST bi-controller, the stability analysis and the observability of the ETV system are studied in the next paragraph.

4.3 Luenberger observers and stability analysis of the ETV system

In order to develop the proposed switching bi-controller based flatness, two models of ETV are given as the state space formulation (25) with matrices $\mathbf{A}_1$,$\mathbf{A}_2$, $\mathbf{B}_1$, $\mathbf{B}_2$, $\mathbf{C}_1$ and $\mathbf{C}_2$ such that

$$\mathbf{A}_1 = \begin{pmatrix} 0 & 1 & 0 \\ 0 & 0 & 1 \\ 0.006152 & -0.9540 & 1.9480 \end{pmatrix} \tag{69}$$

$$\mathbf{A}_2 = \begin{pmatrix} 0 & 1 & 0 \\ 0 & 0 & 1 \\ 0.006152 & -0.9540 & 1.9460 \end{pmatrix} \tag{70}$$

$$\mathbf{B}_1 = \begin{pmatrix} 0 \\ 0 \\ 1 \end{pmatrix} \tag{71}$$

$$\mathbf{B}_2 = \begin{pmatrix} 0 \\ 0 \\ 1 \end{pmatrix} \tag{72}$$

$$\mathbf{C}_1 = \begin{pmatrix} 0.0007376 & 0.01334 & 0.007480 \end{pmatrix} \tag{73}$$

$$\mathbf{C}_2 = \begin{pmatrix} 0.0007376 & 0.01333 & 0.007479 \end{pmatrix} \tag{74}$$

To guarantee the stability of the studied ETV system, LMIs are solved with success. A common Lyapunov function is found for the two switched linear models. Thus, by applying the **Theorem** of subsection 3.3, the ETV system is globally asymptotically stable for the following definite positive matrix P

$$P = 10^{-10} * \begin{pmatrix} 0.2921 & 0.0262 & 0.0637 \\ 0.0262 & 0.1995 & 0.0123 \\ 0.0637 & 0.0123 & 0.0814 \end{pmatrix} \tag{75}$$

and by applying **Lemma** and LMIs of subsection 3.3, the calculated Luenberger observer's gains L_1 and L_2 in closed-loop case, using LMIs, are

$$\mathbf{L}_1 = \begin{pmatrix} 54.5046 \\ 36.8992 \\ -56.7202 \end{pmatrix}, \ \mathbf{L}_2 = \begin{pmatrix} 54.4696 \\ 36.8886 \\ -56.6852 \end{pmatrix} \tag{76}$$

Thus, the Luenberger observer's gains are determined using linear matrix inequalities taking into account the stability of the system based on Lyapunov theory. Then, the observers are used in order to detect and to localize sensor fault occurrence.

By solving LMIs, a common Lyapunov function is found for the switched linear system. Hence, the problem is feasible and the overall system is globally asymptotically stable.

The following paragraph concerns the design of the robust ETV RST bi-controller based-flatness.

4.4 Robust ETV RST bi-controller based-flatness design

Despite relevant studies [13, 14] on the introduction and design of robust controllers, achieving high performance is still a challenging objective. As emphasized in these studies, the significant advantage of the proposed RST based-flatness bi-controller is its robustness, especially, for high frequencies. In fact, the developed control law ensures robustness to external disturbances, attenuation of additive noises and asymptotic tracking of a reference trajectory generated from the flat system. The analysis of the output sensitivity functions makes easy the choice of tuning parameters for the RST based-flatness bi-controller.

Indeed, to guarantee the robustness and the performances of the proposed RST bi-controller based flatness in terms of disturbances rejection and noise attenuation, pre-specified sensitivity functions can be used, [9, 18, 19].

(a) Robust controller design

In order to obtain robust controllers, are introduced the pre-specified parts H_S and H_R given by (77) and (78). The polynomial H_S is used to allow the rejection of the static disturbance of the output signal and the H_R polynomial to eliminate the high frequency noises at the input signal [18, 19, 20, 21].

$$H_S(q^{-1}) = 1 - q^{-1} \tag{77}$$

$$H_R(q^{-1}) = 1 + q^{-1} \tag{78}$$

By taking into account these pre-specified parts, the polynomials of the re-calculated RST bi-controller based flatness can be expressed by

$$\tilde{R}_1(q^{-1}) = H_R(q^{-1})R_1(q^{-1}) \tag{79}$$

$$\tilde{R}_2(q^{-1}) = H_R(q^{-1})R_2(q^{-1}) \tag{80}$$

$$\tilde{S}_1(q^{-1}) = H_S(q^{-1})S_1(q^{-1}) \tag{81}$$

$$\tilde{S}_2(q^{-1}) = H_S(q^{-1})S_2(q^{-1}) \tag{82}$$

The design of the robust RST based-flatness bi-controller is, then, given, in this case for the extended transfer functions $\tilde{H}_1$ and $\tilde{H}_2$, as follows

$$\tilde{H}_1(q^{-1}) = \frac{B_1(q^{-1})H_R(q^{-1})}{A_1(q^{-1})H_S(q^{-1})} \tag{83}$$

$$\tilde{H}_2(q^{-1}) = \frac{B_2(q^{-1})H_R(q^{-1})}{A_2(q^{-1})H_S(q^{-1})} \tag{84}$$

and the RST bi-controllers based flatness are obtained by using the method presented given previously in subsection 3.2.

(b) Sensitivity functions

The sensitivity functions presented below are calibrated and recomputed to ensure the required performance, depending on the type of disturbance to be taken into account. This is done to maintain nominal performance even in the presence of modeling errors and reject disturbances [18].

- The disturbance-output sensitivity functions are

$$S_{yd,1} = \frac{\tilde{A}_1(q^{-1})\tilde{S}_1(q^{-1})}{\tilde{A}_1(q^{-1})\tilde{S}_1(q^{-1}) + \tilde{B}_1(q^{-1})\tilde{R}_1(q^{-1})} \tag{85}$$

$$S_{yd,2} = \frac{\tilde{A}_2(q^{-1})\tilde{S}_2(q^{-1})}{\tilde{A}_1(q^{-1})\tilde{S}_2(q^{-1}) + \tilde{B}_1(q^{-1})\tilde{R}_1(q^{-1})} \tag{86}$$

- And the disturbance-input sensitivity functions are

$$S_{ud,1} = \frac{-\tilde{A}_1(q^{-1})\tilde{R}_1(q^{-1})}{\tilde{A}_1(q^{-1})\tilde{S}_1(q^{-1}) + \tilde{B}_1(q^{-1})\tilde{R}_1(q^{-1})} \quad (87)$$

$$S_{ud,2} = \frac{-\tilde{A}_2(q^{-1})\tilde{R}_2(q^{-1})}{\tilde{A}_2(q^{-1})\tilde{S}_2(q^{-1}) + \tilde{B}_2(q^{-1})\tilde{R}_2(q^{-1})} \quad (88)$$

The study of the robustness of the developed switching RST bi-controller is based on the frequencies analysis of the modules of the various sensitivity functions. Sensitivity functions desired templates are defined through the constraints of imposed performances and tolerated robustness margins.The purpose is to have the disturbance output sensitivity function inside the predefined upper and lower templates. Furthermore, input sensitivity function should have a decreasing shape showing that the proposed switching RST bi-controller based flatness is insensitive to noise.

4.5 Simulation results

The polynomial form for the desired flat trajectory expressed in continuous-time, denoted by $z_j^d(t)$, for $j = \{1, 2\}$, is presented by the following polynomial form

$$z_j^d(t) = \begin{cases} \frac{CONST1}{B_j(1)}, \text{ if } 0 \leq t \leq t_0 \\ POLY_{j,1}(t), \text{ if } t_0 \leq t \leq t_1 \\ \frac{CONST2}{B_j(1)}, \text{ if } t_1 \leq t \leq t_2 \\ POLY_{j,2}(t), \text{ if } t_2 \leq t \leq t_3 \\ \frac{CONST1}{B_j(1)}, \text{ if } t \geq t_3 \end{cases} \quad (89)$$

$CONST1$ and $CONST2$ are constants, $t_0 = 4s$, $t_1 = 7s$, $t_2 = 11s$ and $t_3 = 16s$ are the instants of transitions. For each model, $B_j(1)$ represents the static gain for each operating model. The polynomials $POLY_{j,1}(t)$ and $POLY_{j,2}(t)$ are calculated using the polynomial interpolation technique, [18, 19, 20].
For instance, for $j = 1$: $\theta_{min} \simeq 0.4$ rad and $\theta_{max} \simeq 0.9$ rad, Figure 4 provides the desired output trajectories ${y_1}^d(k)$ and ${y_2}^d(k)$ for each operating model.

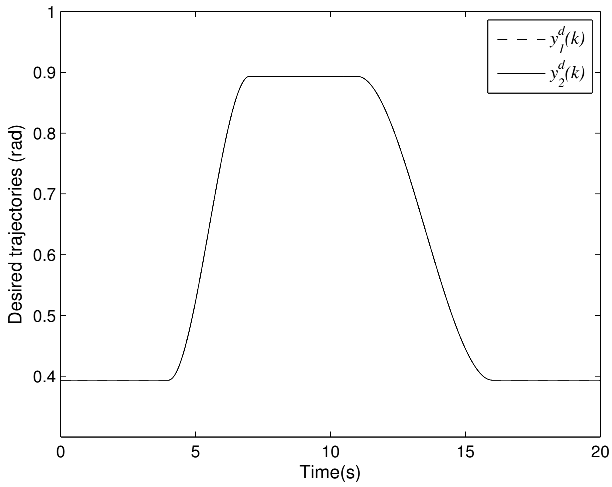

Figure 4: Desired trajectories $y_1^d(k)$ and $y_2^d(k)$

Figure 5 shows that the two disturbance-output sensitivity functions are within the specified robustness templates as desired. Additionally, Figure 6 displays an attenuation in the high frequencies of the disturbance input sensitivity functions by taking values less than 0 db for high frequencies, which indicates that the noise at the input has been eliminated. These observations show that the robustness conditions are satisfied. Consequently, the robustness of the proposed RST switching bi-controller, based flatness in terms of disturbances rejection and noises attenuation , is guaranteed while respecting the predefined robustness templates.

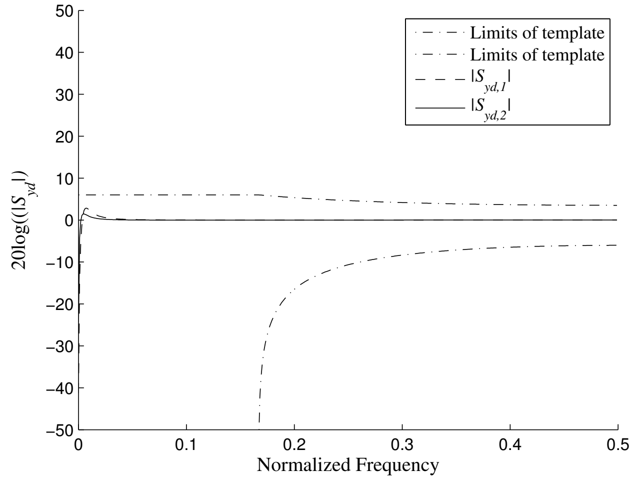

Figure 5: Output sensitivity functions $|S_{yd,j}|$ output disturbances case

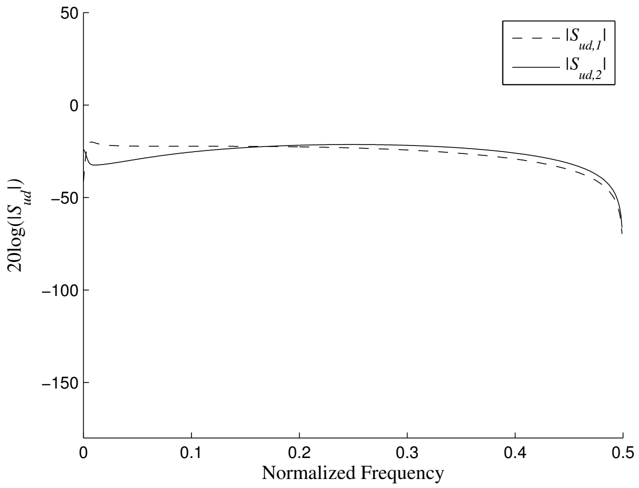

Figure 6: Input sensitivity functions $|S_{ud,j}|$ input disturbances case

Moreover, the performance of the robust switching RST bi-controller based on flatness and on Luenberger observers is shown through simulation results of Figures 7, 8, 9, and 10. In fact, the proposed controller has better dynamic performance and robustness with respect to desired flat trajectory signals even in presence of sensor fault. These results highlight the controller's ability to achieve high-performance desired trajectory tracking by rejection of the sensor fault observed at $t = 9s$. Also, in Figure 10, the residual values indicate that their behaviors changes and, consequently, a fault detection at the time of the sensor fault occurrence. The obtained results show the efficiency of the proposed RST bi-controller based on flatness and on Luenberger observers to the exogenous sensor fault occurrence and the robustness in term of tracking desired flat trajectory.

From the results, it is concluded that the performances of the control strategy are satisfactory. The switching based flatness bi-controller allows the tracking of the desired throttle position with accuracy even in the case of sensor fault occurrence. The proposed controllers accommodate sensor fault properly based on residual values, using stateflow and ensure the stability of ETV system. Notably, Figure 8 shows that the tracking error of the appropriate model is negligible during the transient regime and completely eliminated in the steady-state even in the presence of sensor fault.

The obtained results reflect that the proposed control, using flatness property, effectively performs high performance during dynamic operating conditions. The control law developed guarantees robustness to external disturbances and ensures asymptotic tracking of a reference throttle angle generated from the flat output system. In addition, obtained analysis of the sensitivity functions of the controllers has facilitated the choice of tuning parameters for RST bi-controller based-flatness.

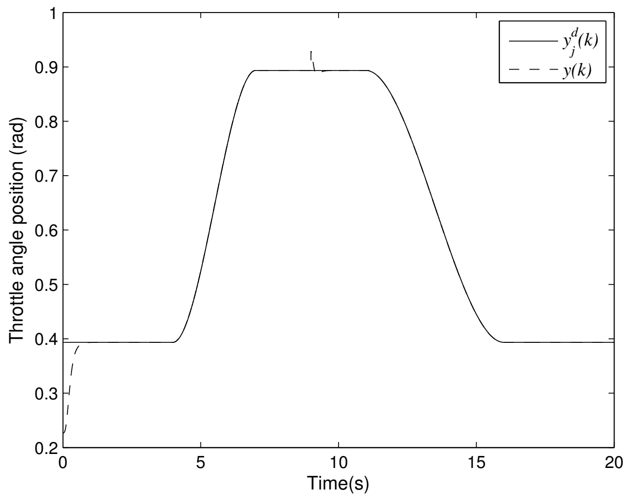

Figure 7: System output signal $y(k)$ and desired output signal $y_j^d(k)$

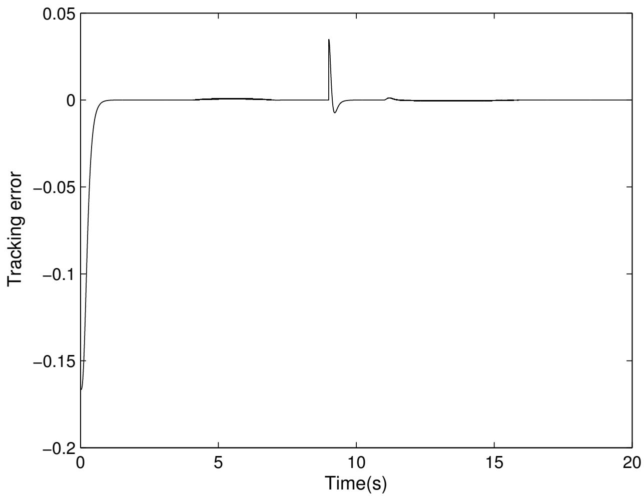

Figure 8: Tracking error $e_j(k)$

5 Conclusion

In this paper, a robust RST bi-controller based on flatness and on Luenberger observers to detect the sensor fault and/or disturbances of the studied Electronic Throttle Valve (ETV) is proposed. The reached performances of the proposed robust bi-controller show that the choice of the closed-loop poles of the tracking dynamics was well designed. Two linear models were identified for the ETV based on its default throttle plate position, and switching between these models was accomplished using stateflow tool based on a comparison of the residues generated by a Luenberger observers. The gains of the observers were obtained by solving a set of LMIs and the system's stability was established by using the Lyapunov theory. Simulation results showed the efficiency of the proposed switching RST

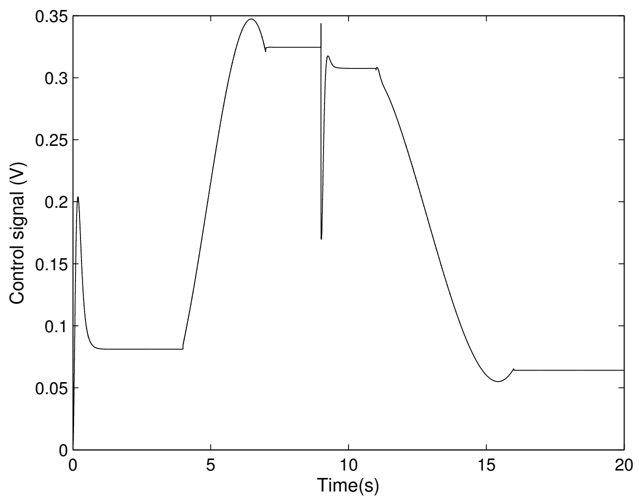

Figure 9: Control signal $u_j(k)$ of the selected active controller

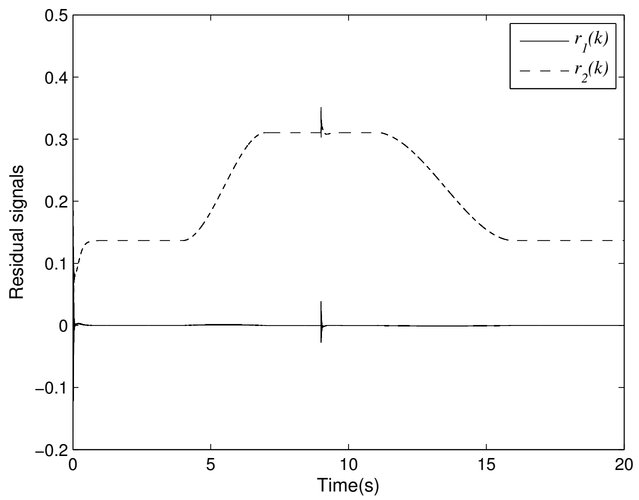

Figure 10: Residual values $r_j(k)$

bi-controller based-flatness in terms of robustness and of tracking of the desired angle flat trajectory, rejecting disturbances and detecting sensor fault.

Nevertheless, for experimental implementation of the proposed control law, the control input signal could exceed the limit values and/or might present discontinuities due to the switching between controllers and consequently the loss of expected performances. In fact, the performances of a transient response to a reference input are measured in terms of overshoot and settling time. Thus, in order to enhance the switching transient response performances, we propose to introduce an Anti-Windup Bumpless Transfer (AWBT) compensators for each controller to minimize the effects of any control input discontinuities and to compensate the overshoot during the switching time on the closed-loop performances which will be suggested in future work. Also, as prospects for our work, we suggest to generalize our proposed approach for multi-controllers as well as the application of the proposed strategy in real-time ETV system control in presence of sensor and/or actuator faults occurrence and variations of system parameters.

References

[1] Acho, L.; Pujol-Vázquez, G.; Gibergans-Báguena, J. (2020). A recent electronic control circuit to a throttle device, *Electronics. 9(1), 191-200*, 2020.

[2] Aidi, I.; Ayadi, M.; Benrejeb, M.; Borne, P. (2010). Flatness-based control of the throttle valve using a neural observer, *Journal of Research and Surveys*, 12, 333-344, 2010.

[3] Alessandri A.; Coletta, P. (2001). Design of Luenberger observers for a class of hybrid linear systems, *Hybrid Systems: Computation and Control, Lecture Notes in Computer Science*, vol. 2034,7-18, 2001.

[4] Amini, M. R.; Razmara, M.; Shahbakhti, M. (2017). Robust model-based discrete sliding mode control of an automotive electronic throttle body, *SAE International Journal of Commercial Vehicles*, 10(1), 317-330, 2017.

[5] Ashok, B.; Ashok, S. D.; Kumar, C. R.; Kavitha, C. (2019). Neural network based virtual sensor for throttle valve position estimation in a SI engine, *International Conference on Advances in Design, Materials, Manufacturing and Surface Engineering for Mobility*, 2019.

[6] Benrejeb, M. (2010). Stability Study of two levels hierarchical nonlinear system, *IFAC Proceedings Volumes*, 43(8), 30-41, 2010.

[7] Benrejeb, M.; Gasmi, M.; Borne, P. (2005). New stability conditions for TS fuzzy continuous nonlinear models, *Nonlinear Dynamics and Systems Theory*, 5(4), 369-379, 2005.

[8] Benrejeb, M. (1980). Sur l'analyse et la synthèse de processus complexes hiérarchisés. Application aux systèmes singulièrement perturbés, *Thèse de Doctorat ès Sciences Physiques, Université des Sciences et Technologie de Lille*, 1980.

[9] Bouallègue, S.; Haggège J.; Benrejeb M. (2011). Particle swarm optimization-based fixed-structure H∞ control design. *International Journal of Control, Automation, and Systems* , 9(2), 258-266, 2011.

[10] Chang, S. C. (2021). Stability analysis and chaos control of electronic throttle dynamical system, *Mathematical Problems in Engineering*, vol. 2021, 1-14, 2021.

[11] Chihi, I.; Abdelkrim, A.; Benrejeb, M. (2015). Multimodel approach to characterize human handwriting motion. *Biological Cybernitics*, 2015.

[12] Deur, J.; Pavkovic, D.; Peric, N.; Jansz, M.; Hrovat, D. (2004). An electronic throttle control strategy including compensation of friction and limp-home effects, *In IEEE Trans. on Industry Applications*, 40, 821-834, 2004.

[13] Dhanasekar, R.; Ganesh Kumar, S.; Rivera, M. (2016). Sliding mode control of electric drives/review, *IEEE International Conference on Automatica (ICA-ACCA)*,1-7, Curico, 2016.

[14] Dulau, M. ; Oltean, S. E., (2020). Simulations of robust control of the throttle valve position, *IEEE International Conference on Automation, Quality and Testing, Robotics (AQTR), 1-5*, 2020.

[15] Elfelly, N.; Dieulot, J.Y.; Benrejeb, M.; Borne, P. (2012). A Multimodel Approach for Complex Systems Modeling based on Classification Algorithms *International Journal of Computers, Communications & Control (IJCCC)*, 7(4), 644-659, 2012.

[16] Fliess, M.; Levine, J.; Martin, P. ; Rouchon, P. (1992). On differentially flat nonlinear systems, *In Proceedings International Federation for Automatic Control (IFAC) - Nonlinear Control System Symposium (NOLCOS)*, 408-413, Design, Bordeaux, 1992.

[17] Gharsallaoui, H.; Gritli, W.; Benrejeb, M. (2016). Robust flatness-based switching reconfiguration control using stateflow machines of electronic throttle valve. *3rd International Conference on Structural Nonlinear Dynamics and Diagnosis (CSNDD)*, Marrakech, 2016.

[18] Gharsallaoui, H.; Ayadi, M.; Benrejeb, M.; Borne, P. (2009). Flatness-based control and conventional RST polynomial control of thermal process. *International Journal of Computers, Communications & Control (IJCCC)*, 4(1), 27-41, 2009.

[19] Gharsallaoui, H.; Ayadi, M.; Benrejeb, M.; Borne, P. (2010) Robust Flatness-based Multi-controllers Approach, *Studies in Informatics and Control*, 1220-1766, 19(4), pp. 357-368, 2010.

[20] Gharsallaoui, H.; Ayadi, M.; Benrejeb, M.; Borne, P. (2013) Comparison of New Flatness-based Switching Reconfiguration Control Approach, *International Conference on Control, Decision and Information Technologies (CoDIT 2013)*, Hammamet, 2013

[21] Gharsallaoui, H.; Ayadi, M.; Benrejeb, M. ; Borne, P. (2010). Flatness-based Switching Control. *The 12th LSS IFAC Symposium on Large Scale Systems: Theory and Applications*, Lille, 2010.

[22] Ghorbel, C.; Abdelkrim, A.; Benrejeb, M. (2010). Observers for continuous nonlinear systems containing unknown parameters and described by Takagi-Sugeno Fuzzy model, *International Journal of Control and Automation*, 3(2), 2010.

[23] Gong, X.; Hu, Y.; Sun, P.; Chen, H. (2012). A nonlinear feedforward-feedback controller design for electronic throttle based on flatness *In the Chinese on Control and Decision Conference (CCDC)*, 1542-1547, Taiwan, 2012.

[24] Gritli, W.; Gharsallaoui, H.; Benrejeb, M. (2018). Electronic throttle valve Takagi-Sugeno fuzzy control based on nonlinear unknown input observers, *International Journal of Computers, Communications & Control, (IJCCC)*, 13(5), 808-823, 2018.

[25] Gritli, W.; Gharsallaoui, H.; Benrejeb, M. (2016). PID-type fuzzy scaling factors tuning using genetic algorithm and simulink design optimization for electronic throttle valve *International Conference on Control, Decision and Information Technologies (CoDIT)*, 216-221, Malta, 2016.

[26] Kasab, P. V.; Chopade, N. B.; Bhagat, S. (2019). Implementation of throttle position sensor for angular movement in automobiles, *5th International Conference on Computing Communication Control and Automation*, Pune, 1-4, 2019.

[27] Khedher, A.; Ben Othman, K.; Benrejeb, M.; Maquin, D. (2010). Adaptative observer for fault estimation in nonlinear systems described by Takagi-Sugeno model, *Control and Automation (MED), 18th Mediterranean Conference*, Marrakech, 261-266, 2010.

[28] Ksouri-Lahmari, M.; Borne, P.; Benrejeb, M. (2004). Multimodel: the construction of model basis. *Studies in Informatics and Control*, 13(3), 199-210, 2004.

[29] Ksouri-Lahmari, M.; El Kamel, A.;Borne, P.; Benrejeb, M. (1997). Multimodel multicontrol decision making in system automation, *Conference on System Man Cybernetics*, 4, 3490-3494, 1997.

[30] Lebbal, M.; Chafouk, H.; Hoblos, G.; Lefebvre, D. (2007). Modelling and identification of nonlinear systems by a multimodel approach: application to a throttle valve. *In Int. Journal Information and Systems Science*, 3, 67-87, 2007.

[31] Manai, Y.; Benrejeb, M. (2011). New condition of stabilization for continuous Takagi-Sugeno fuzzy system based on fuzzy Lyapunov function. *International Journal of Control and Automation*, 4(3), 51–63, 2011.

[32] Prodanovic, J.; Stojic, B. (2019). Control strategy for aftermarker eletronic throttle control, *Mobility and Vehicle Mechanics*, 45(3), 41-50, 2019.

[33] Pujol, G.; Segui, Y. S.; Acho Zuppa, L.; Vargas, A. N. (2015). Asymmetric modelling and control of an electronic throttle, *International Journal of Numerical Modelling Electronic Networks Devices and Fields*, 29(2), 2015.

[34] Sakly, M.; Sakly, A.; Mahjoub, N.; Benrejeb, M. (2009). Optimization Switching instants for optimal control of linear switched system based on genetic algorithms, *IFAC Proceedings Volumes*, 42(19), 249-253, 2009.

[35] Singureanu, M.; Copae, I. (2021). Diagnosis of gasoline injection engine and fault tolerant control, *International Journal for Research in Applied Science and Engineering Technology (IJRASET)*, 9(7), 23, 2021.

[36] Song, D.; Li Y.(2020). Study on composite control strategy of transient air-fuel ratio for gasoline engine based on model, *IOP Conference Series: Earth and Environmental Science*, 513(1), 27–33, 2020.

[37] Thakur, A .(2019). An overview of “drive by wire” technology for automobiles, *Amity University IEEE Conference*, London, 2019.

[38] Vasak, M.; Baotic, M.; Petrovic, I.; Peric, N. (2007). Hybrid theory-based time-optimal control of an electronic throttle. *IEEE Trans. on Industrial Electronics*, 54, 1483-1494, 2007.

[39] Xue J.; Jiao X. (2021). Barrier Lyapunov function-based adaptive backstepping control for electronic throttle control system, *Transportmetrica A: Transportation Science*, 17(1), 59–80, 2021.

[40] Yang, C. (2004). Model-based analysis and tuning of electronic throttle controllers. *Visteon Corporation, SAE World Congress Detroit*, 63-65-67, Michigan, 2004.

[41] Yuan, X. F.; Wang, Y. N; Sun, W; Wu, L. H. (2010). RBF networks-based adaptive inverse model control system for electronic throttle. *IEEE Trans. on Control Systems Technology*, 18, 750-756, 2010.

[42] Zhang, J.; Li, J. (2018). Adaptive backstepping sliding mode control for wheel slip tracking of vehicle with uncertainty observer. *Measurement and Control Control*, 51(9–10), 396–405, 2018.

Cite this paper as:

Gharsallaoui, H.; Gritli, W.; Benrejeb, M.; Borne, P. (2023). RST Switching Bi-controller Based Flatness for an Electronic Throttle Valve, *International Journal of Computers Communications & Control*, 18(5), 5630, 2023. https://doi.org/10.15837/ijccc.2023.5.5630